Program Digest, 2019 IEEE International Ultrasonics Symposium (IUS)
Glasgow, Scotland, October 6-9, 2019

Atherosclerotic carotid bifurcation phantoms with a stenotic soft inclusion for flow-structure ultrasound imaging analysis

Boris Chayer
Laboratory of Biorheology and Medical Ultrasonics,
University of Montréal Hospital Research Center (CRCHUM),
Montréal, QC, Canada
boris.chayer@crchum.qc.ca

Marcel van den Hoven
Department of Biomedical Engineering,
Eindhoven University of Technology,
Eindhoven, Netherlands

Marie-Hélène Roy Cardinal
Laboratory of Biorheology and Medical Ultrasonics,
University of Montréal Hospital Research Center (CRCHUM),
Montréal, QC, Canada

Hongliang Li
Laboratory of Biorheology and Medical Ultrasonics,
University of Montréal Hospital Research Center (CRCHUM),
Montréal, QC, Canada

Craig Madiena
Laboratory of Biorheology and Medical Ultrasonics,
University of Montréal Hospital Research Center (CRCHUM),
Montréal, QC, Canada

Abigail Swillens
IBiTech-bioMMeda,
Ghent University,
Ghent, Belgium

Richard Lopata
Department of Biomedical Engineering,
Eindhoven University of Technology,
Eindhoven, Netherlands

Guy Cloutier
Laboratory of Biorheology and Medical Ultrasonics
University of Montréal Hospital Research Center (CRCHUM),
Montréal, QC, Canada
guy.cloutier@umontreal.ca

***Abstract*— As the complexity of ultrasound signal processing algorithms increases, it becomes more difficult to demonstrate their added value. In the context of quantitative measurements such as vascular elastography, vector flow mapping, and ultrafast tissue Doppler, innovative validation strategies are required. Phantoms have been widely used but they do not correspond to the geometry of vulnerable carotid atherosclerotic plaques containing a large lipid pool embedded within the vessel wall of an anthropomorphic lumen geometry.**

We propose a method of manufacturing such phantoms for applications in flow imaging and elastography. The internal carotid geometry was based on a computed tomography scan of a healthy individual. During the fabrication process, a soft inclusion mimicking a stenotic lipid pool was embedded within the vascular wall. The phantom wall and soft inclusion were made of polyvinyl alcohol (PVA) that undergone different numbers of freezing-thawing cycles to produce different mechanical property.

Mechanical testing measured Young's moduli of the vascular wall and soft inclusion at 342 ± 25 kPa and 17 ± 3 kPa, respectively. Strain elastography results on the lipid pool mimicking inclusion, fibrous cap and remaining phantom wall showed greater strain in the lipid pool, which is consistent with expected results. Because of their realistic geometries and mechanical properties, those phantoms may become advantageous for fluid-structure experimental studies and validation of new ultrasound-based imaging technologies.

Keywords—Elastography, atherosclerosis, ultrasound vascular phantom, Doppler imaging

I. Introduction

By considering the increasing number of complex medical imaging methods being reported in the literature, there is a need for sophisticated validation methods. In response to these needs, and especially in the context of new ultrasound elastography and flow imaging methods being developed, we designed a carotid artery flow phantom with a soft inclusion. The proposed method constitutes a significant step when compared with previous vascular phantoms we developed for ultrasound imaging [1 – 5].

Among carotid artery phantoms proposed in the literature for ultrasound applications, several rectilinear designs [6 - 9] where constructed. More realistic carotid bifurcation phantoms for fluidic *in vitro* studies have also been reported [10 - 12]. However, none of them have focused on designing a plaque having heterogeneous mechanical properties.

The objective of this study was to develop a phantom including a realistic 3D carotid bifurcation with a mimicking vulnerable atherosclerotic plaque. The phantom was designed to include a soft inclusion and a mimicking fibrous cap with different elasticity. Details can be found in [13].

II. Anthropomorphic Phantom Design

A. Mechanical properties

The phantom features elastic properties similar to atherosclerosis arteries, and it was made to be compatible for ultrasound imaging. It was constructed with polyvinyl alcohol cryogel (PVA) experiencing different numbers of freeze-thaw cycles [14]. PVA is known to polymerize when it undergoes freezing and thawing cycles. The phantom characteristics included a severe stenosis, a wall and a fibrous cap with an elasticity of 342 kPa, and a soft inclusion with an elasticity of 17 kPa.

B. Phantom mold design

To design the shape of the phantom, we started with an anthropomorphic carotid geometry based on a CT-scan rendering [15]. This virtual geometry was modified to produce the lumen stem, which allowed to reproduce the lumen of the vessel phantom. The modification was inspired by the morphology of a vulnerable plaque to shape a severe stenosis into the lumen geometry at the bifurcation site. The goal was not to reproduce only the carotid shape and stenosis grade but also the elasticity of the plaque components. Thus, the mold was designed specifically to allow manufacturing a soft inclusion and a thin fibrous cap.

As depicted in Fig. 1, the mold was made of 3 parts, namely 2 halves of the outer mold (blue) and the Y shaped lumen stem that allowed producing the lumen of the phantom (white). All parts were 3D printed in ABS. In order to fabricate the soft inclusion, the outer mold was designed with a small plastic piece (shaped like a lemon seed, green part in Fig. 1) that kept the PVA from filling outside of the plaque compartment during the injection. This small piece was held in place in the void of the plaque compartment by a filling duct. The phantom was prepared with 2 consecutive PVA injections, the first injection allowed to produce the vessel wall and the fibrous cap, and the second was intended to form the softer inclusion.

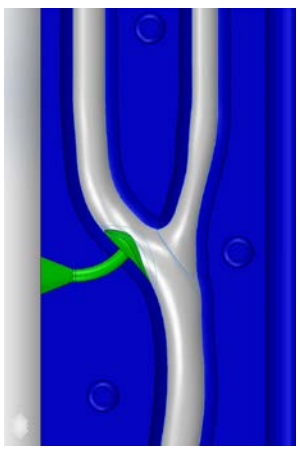

Fig. 1. Details of the designed mold for the manufacturing of an atherosclerotic carotid bifurcation phantom with a stenotic soft inclusion. In blue, one of the outer mold halve. In white, the lumen stem that shaped the lumen of the vessel. In green, the small inclusion plastic piece that formed a cavity into the phantom wall for the soft inclusion.

C. *Phantom manufacturing*

This section describes step by step the approach used to fabricate the vascular phantom. First, we position the lumen stem inside the outer mold. The 2 halves of the outer mold are then closed and sealed together with hot glue. A funnel allow pouring the PVA into the mold by an injection duct until the PVA overflow. The mold is then put in a programmable freezer to undergo 5 freeze and thaw cycles. Every cycle last 24 hours. After 5 cycles, the mold is opened by taking great care to leave the phantom in the back halve. With a scalpel, we then cut the casting duct that support the small plastic piece into the plaque compartment. At this stage, the plastic piece is trapped into the phantom wall. Thanks to the PVA gel deformability, we then remove it gently with tweezer. Then, we fill the plaque compartment with a 2nd injection of PVA and put the phantom into the freezer for a last freeze and thaw cycle. At this point, the lumen stem remains stock in the vessel phantom. To remove it, we break the stem at the weakest bifurcation stenotic site to gently remove each branch of the mimicking carotid artery. It is important to avoid tearing the wall with the sharp broken edges. More details on the fabrication process with supporting images can be found in [13].

III. *IN VITRO* RESULTS

A. *In vitro setup*

To test the performance of the vascular phantom in the context of non-invasive vascular elastography (NIVE) imaging [16], the mimicking carotid artery was introduced into a box filled with degassed water. The rigid box allowed to fix all extremities of the phantom to preserve its original shape. A pulsatile pump was used to circulate a blood mimicking fluid. Ultrasound images were acquired with a research scanner providing access to RF signals (SonixTouch, BK Medical, Peabody, MA, USA).

B. *Elasticity of plaque components*

Figure 2 shows the plaque component segmentation made manually on a phantom B-mode image, and the overlaid NIVE axial strain map obtained with the implementation described in [17]. One could see the phantom vessel wall, the lipidic inclusion and the fibrous cap showing different strain values.

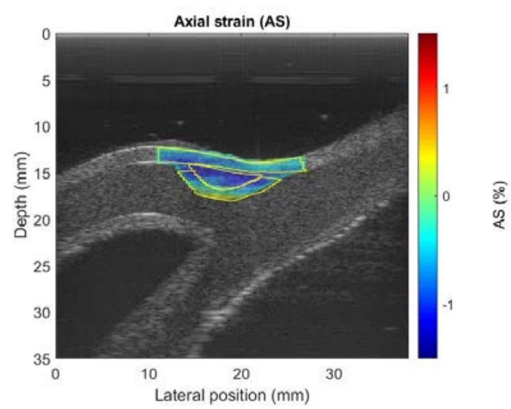

Fig. 2. B-mode and axial strain image of the atherosclerotic carotid bifurcation phantom. The manual segmentations of the plaque regions are also shown with the yellow overlay.

All 3 regions of the plaque that were manually segmented in Fig. 2 were further considered to study locally the time-varying behavior of the axial strain. Figure 3 shows the axial strain averaged over each plaque region over time during the pulsation of the fluid circulated by the pump. In this graph, we clearly see that the lipid pool (the green trace) sustains larger deformation over time than the stiffer wall and fibrous cap. This observation is relevant and means that the NIVE algorithm allows to measure the elastic property of all plaque components including the small inclusion (10 × 5 × 3 mm).

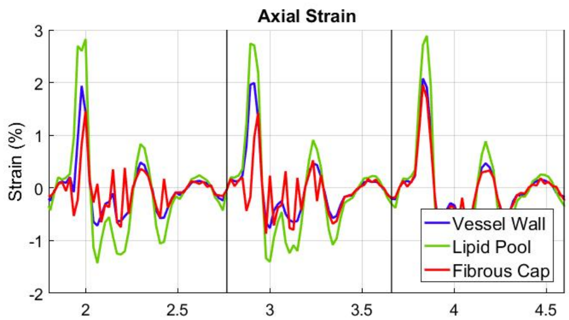

Fig. 3. Percentage of axial strain averaged over each plaque region and traced over time during the pump pulsation.

IV. Discussion and Conclusion

If PVA remains widely used for vascular phantom fabrication, the realism of the 3D shape and mechanical properties must continue to be improved. By introducing a manufacturing process able to reproduce a soft inclusion into the wall of a carotid bifurcation phantom, we could contribute to the development of new ultrasound vascular and tissue rheology methods. As an example, this phantom was recently used to assess the robustness of a NIVE algorithm in the context of out-of-plane motion artifacts [18]. Out-of-plane motions from 0 to 3 mm were studied and it was shown that displacements of 2 mm or less did not affect the strain and shear components of this vascular elastography method.

In conclusion, in the context of an *in vitro* validation with the proposed vascular phantom, the results of this study are suggesting that the NIVE resolution is currently sufficient to discriminate between a plaque inclusion and the fibrous cap. It is believed that this manufacturing process will help phantom designers to produce more realistic 3D geometries with embedded inclusions, for a better match with technology validation needs. Another important contribution of this work is to provide to the scientific community a tool for validating fluid-structure ultrasound imaging technologies in the context of new developments in ultrafast high-resolution imaging.

Acknowledgments

This work was supported by the Collaborative Health Research Program of the Natural Sciences and Engineering Research Council of Canada (CHRP-462240-2014) and the Canadian Institutes of Health Research (CPG134748).

References

[1] Allard, L., Cloutier, G., Durand, L.G., (1995) Doppler velocity ratio measurements evaluated in a phantom model of multiple arterial disease. *Ultrasound Med. Biol., 21 (4):* 471-480.

[2] Brunette, J., Mongrain, R., Cloutier, G., Bertrand, M., Bertrand, O.F., Tardif, J.C., (2001) A novel realistic three-layer phantom for intravascular ultrasound imaging, *Int. J. Cardiac Imaging*, *17 (5):* 371-381.

[3] Cloutier, G., Soulez, G., Qanadli, S.D., Teppaz, P., Allard, L., Qin, Z., Cloutier, F., Durand, L.G., (2004) A multimodality vascular imaging phantom with fiducial markers visible in DSA, CTA, MRA and ultrasound, *Medical Physics*, *31(6)*: 1424-1433.

[4] Allard, L., Soulez, G., Chayer, B., Treyve, F., Qin, Z., Cloutier, G., (2009) Multimodality vascular imaging phantoms: A new material for the fabrication of realistic 3D vessel geometries, *Medical Physics*, *36 (8):* 3758-3763.

[5] Allard, L., Soulez, G., Chayer, B., Qin, Z., Roy, D., Cloutier, G., (2013) A multimodality vascular imaging phantom of an abdominal aortic aneurysm with a visible thrombus, *Medical Physics*, *40 (6):* 063701(1)-063701(10).

[6] Nayak, R., Schifitto, G., & Doyley, M. M. (2017). Noninvasive carotid artery elastography using multielement synthetic aperture imaging: Phantom and *in vivo* evaluation. *Medical physics*, *44*(8), 4068-4082.

[7] Yau, O., Hétu, M. F., Herr, J. E., Adams, M. A., & Johri, A. M. (2018). Development of a carotid vulnerable plaque phantom model evaluated by pixel distribution analysis. *Ultrasound in Medicine & Biology*, *44*(12), 2768-2779.

[8] Perrot, V., Petrusca, L., Bernard, A., Vray, D., & Liebgott, H. (2017). Simultaneous pulse wave and flow estimation at high-framerate using plane wave and transverse oscillation on carotid phantom. In *2017 IEEE International Ultrasonics Symposium (IUS)* (pp. 1-4).

[9] Chee, A. J., Yiu, B. Y., Ho, C. K., & Yu A. C. H. (2018). Arterial phantoms with regional variations in wall stiffness and thickness. *Ultrasound in Medicine & Biology*, *44*(4), 872-883.

[10] Fekkes, S., Saris, A. E., Nillesen, M. M., Menssen, J., Hansen, H. H., & de Korte, C. L. (2018). Simultaneous vascular strain and blood vector velocity imaging using high-frequency versus conventional-frequency plane wave ultrasound: A phantom study. *IEEE Transactions on Ultrasonics, Ferroelectrics, and Frequency Control*, *65(7),* 1166-1181.

[11] Niu, L., Zhu, X., Pan, M., Derek, A., Xu, L., Meng, L., & Zheng, H., (2018). Influence of vascular geometry on local hemodynamic parameters: phantom and small rodent study. *Biomedical Engineering Online*, *17*(1), 30.

[12] O'Flynn, P. M., Roche, E. T., & Pandit, A. S. (2005). Generating an *ex vivo* vascular model. *Asaio Journal*, *51*(4), 426-433.

[13] Chayer, B., van den Hoven, M., Roy Cardinal, M. H., Li, H., Swillens, A., Lopata, R., & Cloutier, G. (2019). Atherosclerotic carotid bifurcation phantoms with stenotic soft inclusions for ultrasound flow and vessel wall elastography imaging. *Physics in Medicine & Biology*, *64*(9), 095025.

[14] Fromageau, J., Gennisson, J.L., Schmitt, C., Maurice, R.L., Mongrain, R., Cloutier, G., (2007). Estimation of polyvinyl alcohol cryogel mechanical properties with four ultrasound elastography methods and comparison with gold standard testings, *IEEE Transactions on Ultrasonics, Ferroelectrics, and Frequency Control*, *54 (3)*: 498-509.

[15] Swillens, A., Løvstakken, L., Kips, J., Torp, H., Segers, P. (2009). Ultrasound simulation of complex flow velocity fields based on computational fluid dynamics. *IEEE Transactions on Ultrasonics, Ferroelectrics, and Frequency Control*, 56(3), 546-556.

[16] Maurice, R. L., Daronat, M., Ohayon, J., Stoyanova, E., Foster, F. S., & Cloutier, G. (2005). Non-invasive high-frequency vascular ultrasound elastography. *Physics in Medicine & Biology*, *50*(7), 1611-1628.

[17] Mercure, E., Destrempes, F., Roy Cardinal, M.H., Porée, J., Soulez, G., Ohayon, J., Cloutier, G. (2014). A local angle compensation method based on kinematics constraints for non-invasive vascular axial strain computations on human carotid arteries, *Computerized Medical Imaging and Graphics*, Special issue paper, *38 (2):* 123-136.

[18] Li H., Chayer B., Roy Cardinal M.H., Muijsers J., van den Hoven M., Qin Z., Gesnik M., Soulez G., Lopata R.G.P., Cloutier G., (2018). Investigation of out-of-plane motion artifacts in two-dimensional noninvasive vascular ultrasound elastography, *Physics in Medecine & Biology., 63*: 245003(1)-(15).